

## The Crystal Structure of Lead Ethylxanthate

By HITOSI HAGIHARA

*The Institute of Physical and Chemical Research, Komagome, Bunkyo-ku, Tokyo, Japan*

AND SHUJI YAMASHITA

*Tokyo Metropolitan Isotope Research Center, Fukazawa-cho, Setagaya-ku, Tokyo, Japan*

(Received 27 October 1965 and in revised form 24 January 1966)

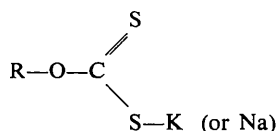
Lead ethylxanthate,  $\text{Pb}(\text{SSCOCH}_2\text{CH}_3)_2$ , is monoclinic with

$$a = 13.267 \pm 0.016, b = 4.301 \pm 0.015, c = 22.722 \pm 0.016 \text{ \AA}; \beta = 109^\circ 16' \pm 5';$$

the space group is  $P2_1/c$  and  $Z=4$ . Through the dithiocarbonic ends the two xanthate groups are bonded with the lead atom, with a bond angle of  $98.2^\circ \pm 0.9^\circ$ . The molecule is not planar, although each xanthate group, ignoring the hydrogen atoms, is almost planar. It does not possess a twofold rotation axis passing through the lead atom and it forms an asymmetric unit in the structure. A geometrical interpretation is given of the asymmetrical molecular structure in terms of the rotations of the molecular segments around Pb-S, C-S and O-S single bonds in the crystalline state. The molecules are bound together through van der Waals forces between double-bonded sulphur atoms and between methyl ends of the alkyl groups.

### Introduction

Crystal structure analysis of the heavy metal salts of xanthic acid, the *O*-ester of dithiocarbonic acid, is important in relation to the mechanism of 'collection' in the technical process of separating sulphide minerals by flotation (Taggart, 1947). The potassium and sodium salts of xanthic acid with the structural formulae



where R is an alkyl group, are most commonly used in this process as collectors. They dissociate in water into  $(\text{ROCSS})^-$  and  $\text{K}^+$  (or  $\text{Na}^+$ ) ions. The interaction of the above anion with sulphide mineral surfaces in water has been a problem of intensive studies and of much debate relating to the flotation mechanism (Wark & Sutherland, 1955; Gaudin, 1957).

One of us previously studied the behaviour of several kinds of alkyl xanthates on fresh and oxidized cleavage faces of galena, PbS, by the reflexion method of electron diffraction (Hagihara, 1952). This technique was proved to be useful in determining the molecular array of adsorbates in a monolayer produced on the cleavage surface (Hagihara & Uchikoshi, 1954), or in the identification and the orientation determination of oxidation and other reaction products which are formed on mineral surfaces before and after reaction with xanthate solutions (Hagihara, Uchikoshi & Yamashita, 1957; Hagihara, Sakurai & Ikeda, 1964). It has been supposed that the interaction of xanthate anions in the solution with the lead cations in the solution or at

the uppermost layer of the crystal surface plays a most important role in the reactions. The present analysis concerns the determination of the molecular structure of lead ethylxanthate,  $\text{Pb}(\text{SSCOCH}_2\text{CH}_3)_2$ , in its crystalline state, as a step to elucidate the nature of the binding force between the heavy metal cation and sulphidic collector anion.

### Experimental

Lead ethylxanthate powder was prepared from the white precipitate obtained on titration of aqueous solutions of purified potassium ethylxanthate and lead nitrate. The precipitate was filtered and dehydrated in a vacuum desiccator. The obtained powder was dissolved in acetone or ethyl alcohol, and single crystals of lead ethylxanthate were obtained by slow precipitation from the solution. The grown crystals were usually thin needle shaped with cross section forming a parallelogram making an angle of about  $109^\circ$ . From Laue photographs the crystal was determined to be monoclinic,  $2/m$ , with the long axis parallel to the *b* axis. Very rarely, tiny crystals bipyramidal in shape, 0.5 mm long in the *b*-axis direction and 0.1 mm  $\times$  0.1 mm in cross section at the base, were obtained. In the diffraction work a needle crystal 0.1 mm  $\times$  0.1 mm in cross section was used for the *b*-axis setting and a bipyramidal crystal for the *a*-axis setting. The crystals were practically stable in air at room temperatures.

A series of multiple film Weissenberg photographs of the  $k=0, 1, 2$  and 3 layers of a *b*-axis oriented crystal and the  $h=0$  layer of an *a*-axis oriented crystal were taken at room temperatures with filtered Cu  $K\alpha$  radiation by the equi-inclination method. They revealed a monoclinic unit cell with

$$a = 13.267 \pm 0.016, b = 4.301 \pm 0.015,$$

$$c = 22.722 \pm 0.016 \text{ \AA}; \beta = 109^\circ 16' \pm 5'.$$

The space group indicated by the systematic extinction is  $P2_1/c$  (No.14); four molecules per unit cell give a calculated density of  $2.42 \text{ g.cm}^{-3}$ . The linear absorption coefficient  $\mu$  came out to be 336. The spacings were measured from the  $h0l$  and  $0kl$  Weissenberg photographs obtained from the crystal coated with a thin layer of aluminum powder, 99.995% in purity, as a reference material.

The intensities were measured with these films by visual comparison with a standard scale. Concerning the zero layer of a  $b$ -axis oriented crystal, a series of photographs was also taken under timed exposures of 1, 3, 9, 27 and 81 hr. For the  $h0l$  and  $0kl$  reflexions the absorption correction for the rhombus shaped cross section was made approximately by the graphical

method (Albrecht, 1939; Howells, 1950). Measured intensities ranged from 3500 to 1. Unobserved reflexions were given numerical values corresponding to half the minimum of the observed intensities in each layer photograph. The intensities were corrected for the Lorentz and polarization factors. The ideal intensities,  $|F|^2$ , ranged from 400 to 1. Corrections for the extinction effects were considered at the final stage of refinement.

### Determination of the structure

#### Patterson functions

$P_0(xz)$  was calculated with 372  $h0l$  terms including 28 zeros (93%) obtained up to  $2 \sin\theta = 1.98$ . Two sheets of  $P_0(xz)$  maps were overlaid with each other, the origin of one sheet being superimposed on a predominant peak of a lead-lead vector in the other sheet, and the product of the two maps was evaluated at the  $30 \times 30$

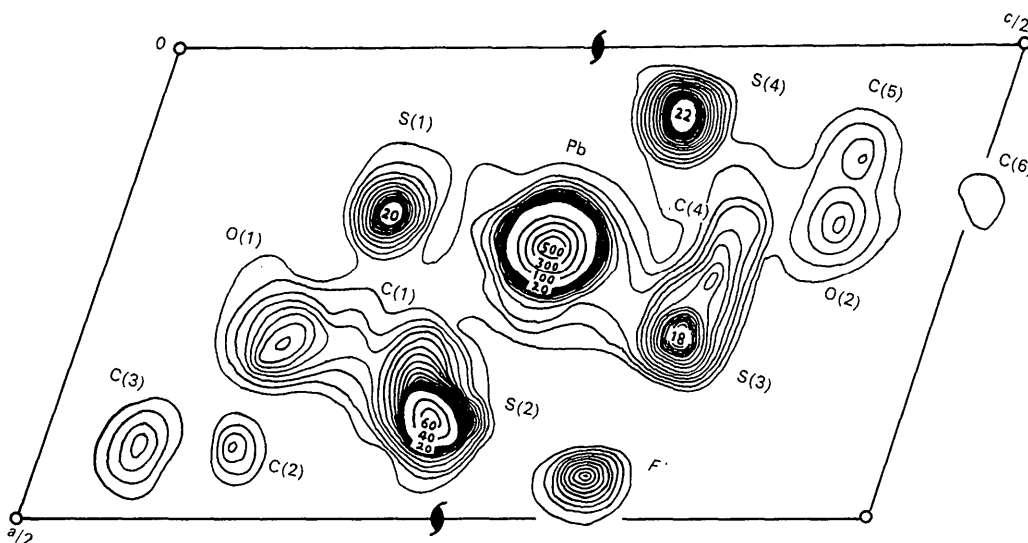


Fig. 1. Shifted Patterson product. Projection on (010).

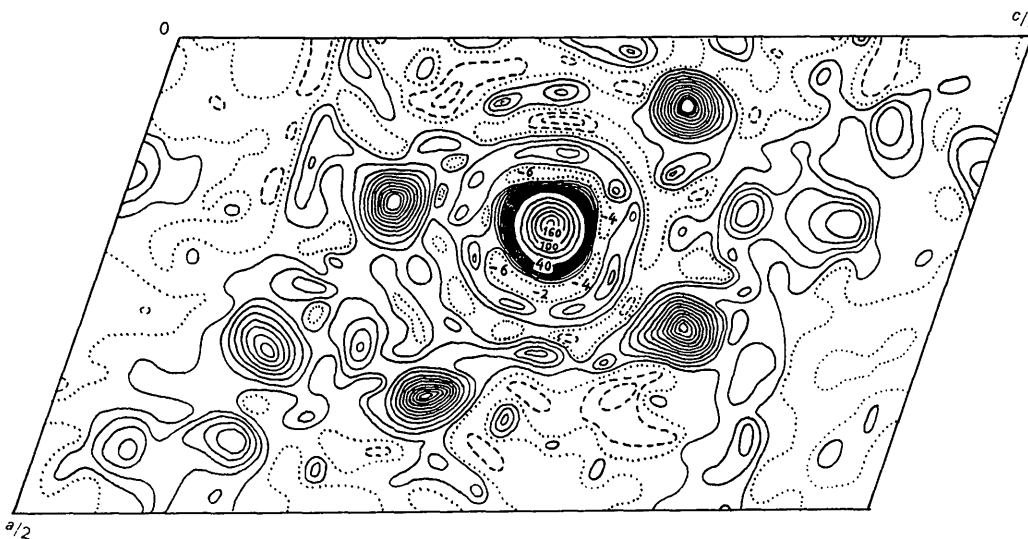


Fig. 2. (010) electron-density projection, with contours at intervals of  $2 \text{ e.}\text{\AA}^2$ , except the lead atom.

points. The result at once revealed the projection of a lead ethylxanthate molecule on (010), as shown in Fig. 1, without confusing overlappings for lead, sulphur, oxygen and carbon atoms. A peak designated as *F* in Fig. 1 is caused accidentally by superimposition of the non-vanishing slopes of the contours surrounding two sulphur atoms. Distortion in shape and abnormally high contour values around S(2) are due to the disturbing effect of the non-vanishing slope of contours for the lead atom in one sheet on the contours of the sulphur atom in the other.

Generalized Patterson functions,  $P_1(xz)$  and  $P_2(xz)$ , were calculated with 698 *h1l* terms including 144 zeros (79%) and 628 *h2l* terms including 240 zeros (62%), respectively. By comparing the relative height of peaks in  $P_0(xz)$ ,  $P_1(xz)$  and  $P_2(xz)$ , the approximate  $|y|$  values

for the lead, sulphur, oxygen and carbon atoms were determined. The distinction between  $y$  and  $\bar{y}$  for each atom was judged from the approximate shape of the  $-\text{SSCOCH}_2\text{CH}_3$  group, taking account of the atomic radii and bond angles of the constituent atoms (Pauling, 1960; Landolt-Börnstein, 1955). From the  $y$  coordinate of lead atoms in the unit cell the twofold screw axes and inversion points in the (010) projection were located as shown in Fig. 1.

#### Projection on (010)

Fourier summation was made with 344 observed *h0l* reflexions. The signs of the structure factors were determined from the contribution of the lead atom alone. The parameter of the lead atom was refined through inspection of the map obtained. Fig. 2 shows the map

Table 1. Atomic parameters of lead ethylxanthate,  $\text{Pb}(\text{SSCOCH}_2\text{CH}_3)_2$

Atom		$\sigma$	$B$	$ \Delta x_i /\sigma(x_i)$ in the final cycle of refinement	$\Delta B$ in the final cycle of refinement	
Pb	<i>x</i>	0.2019	0.0039 Å	2.4 Å <sup>2</sup>	0.5	0.12
	<i>y</i>	0.606	0.0035		0.8	
	<i>z</i>	0.2555	0.0050		0.0	
S(1)	<i>x</i>	0.174	0.026	2.3	0.2	0.07
	<i>y</i>	0.20	0.032		0.3	
	<i>z</i>	0.158	0.023		0.1	
S(2)	<i>x</i>	0.384	0.027	2.5	0.4	-0.09
	<i>y</i>	0.51	0.034		0.6	
	<i>z</i>	0.218	0.024		0.1	
S(3)	<i>x</i>	0.306	0.030	2.8	0.2	0.19
	<i>y</i>	0.20	0.037		0.9	
	<i>z</i>	0.352	0.026		0.0	
S(4)	<i>x</i>	0.072	0.029	2.7	0.2	0.16
	<i>y</i>	0.23	0.035		1.2	
	<i>z</i>	0.313	0.025		0.1	
O(1)	<i>x</i>	0.33	0.07	2.4	0.4	0.06
	<i>y</i>	0.19	0.09		0.3	
	<i>z</i>	0.12	0.07		0.0	
O(2)	<i>x</i>	0.20	0.09	3.3	0.5	0.17
	<i>y</i>	0.01	0.11		0.3	
	<i>z</i>	0.42	0.08		0.1	
C(1)	<i>x</i>	0.30	0.10	2.3	0.7	0.13
	<i>y</i>	0.29	0.13		0.1	
	<i>z</i>	0.16	0.09		0.0	
C(2)	<i>x</i>	0.44	0.12	3.1	0.5	0.26
	<i>y</i>	0.26	0.15		0.0	
	<i>z</i>	0.11	0.11		0.0	
C(3)	<i>x</i>	0.43	0.20	5.1	0.0	0.73
	<i>y</i>	0.19	0.22		1.3	
	<i>z</i>	0.05	0.17		0.2	
C(4)	<i>x</i>	0.19	0.10	2.2	0.2	0.18
	<i>y</i>	0.14	0.12		0.6	
	<i>z</i>	0.37	0.09		0.1	
C(5)	<i>x</i>	0.10	0.15	3.9	0.5	0.54
	<i>y</i>	-0.08	0.17		0.2	
	<i>z</i>	0.43	0.13		0.1	
C(6)	<i>x</i>	0.14	0.13	3.2	0.1	0.39
	<i>y</i>	-0.21	0.15		0.2	
	<i>z</i>	0.50	0.11		0.2	

which is finally obtained by applying the usual procedure of successive refinement, taking account of the contributions of all the atoms except hydrogen atoms. The atomic scattering factors used in the calculation were those in *Internationale Tabellen* (1935).

Since, however, the maximum electron density of the lead atom in Fig. 2, attaining almost  $160 \text{ e.}\text{\AA}^{-2}$ , is too high for the precise determination of its parameters, and further the map shows a strong diffraction effect caused by the lead atom, an  $(F_o - F_c)$  synthesis was carried out in order to determine the  $xz$  parameters of the sulphur atoms and of the lead atom more precisely. After six cycles of refinement with an overall isotropic temperature factor the lead and sulphur atoms stood at the saddle points of the electron density contours of the  $(F_o - F_c)$  synthesis. The final reliability index  $R$  was 0.10 with the temperature factor  $B$  at  $1.9 \text{ \AA}^2$ . The parameters  $\sigma(\rho_o)$  and  $\sigma(x_n)$  for the (010) projection are as follows:

$$\begin{aligned} \sigma(\rho_o) &= 1.1 \text{ e.}\text{\AA}^{-2}, \\ \sigma(x) \text{ and } \sigma(z); & \text{ Pb } 0.002 \text{ \AA}, \text{ S } 0.015 \text{ \AA}, \\ & \text{ O } 0.04 \text{ \AA}, \text{ C } 0.06 \text{ \AA}. \end{aligned}$$

#### Projection on (100)

From generalized Patterson functions the  $y$  parameter of the lead atom was determined to be 0.59. The signs of structure factors for the  $0kl$  reflexions were determined at the outset by taking account of the contributions of the lead atom only. Successive Fourier syntheses were carried out with 101 observed  $0kl$  reflexions. A difference Fourier map with the lead atom subtracted is shown in Fig. 3. Because there are overlappings of a pair of sulphur and carbon atoms and a pair of oxygen and carbon atoms, the  $y$  parameters of these atoms must inevitably contain some ambiguities and are still not conclusive. The final  $R$  value for this projection was 0.11, with  $B = 1.9 \text{ \AA}^2$ .  $\sigma(\rho_o)$  and  $\sigma(y)$  for the (100) projection are as follows:

$$\sigma(\rho_o) = 1.4 \text{ e.}\text{\AA}^{-2}$$

$$\sigma(y): \text{ Pb } 0.004, \text{ S } 0.03, \text{ O } 0.08, \text{ C } 0.10, 0.15 \text{ \AA}$$

The comparison of  $F_o$  and  $F_c$  for the  $0kl$  reflexions is shown in Table 2(b). The accuracy in electron density and atomic parameters is a little lower than in the (010) projection.

#### Three-dimensional least-squares refinement

Based on the atomic parameters and temperature factors determined by the (010) and (100) projections, a three-dimensional least-squares refinement was carried out with  $h0l$ ,  $h1l$ ,  $h2l$  and  $h3l$  reflexions totalling to 2220 in number, of which 578 reflexions were unobserved (observed: 74%) and were given half the minimum intensity of observed reflexion in each level. The interlevel correction for the intensity was made by comparing the  $00l$ ,  $01l$ ,  $02l$  and  $03l$  reflexions. Absorption errors were minimized by the use of a thinner needle crystal of  $0.05 \text{ mm} \times 0.05 \text{ mm}$  in cross section.

After five cycles of refinement by ERBR-1 (Van den Hende, 1961) with 2220 reflexions of equal weight, the  $R$  value came out to be 0.180, while with 1642 observed reflexions only it came out to be 0.156. The atomic parameters, isotropic temperature factor for each atom, standard deviations of atomic parameters in  $\text{\AA}$  and the parameter shifts in the final cycle of computation are tabulated in Table 1.

Through this refinement procedure the  $x, z$  parameters have been essentially unchanged from the values determined from the (010) projection, while the  $y$  parameters of Pb, S(1), S(2) and C(3) atoms have changed by amounts larger than their standard deviations. The three-dimensional least-squares refinement was effective in improving the  $y$  parameters determined by the unfavourable (100) projection. The overall  $R$  value, 0.180, however, was worse than the values 0.10 for the (010) and 0.11 for the (100) projection.

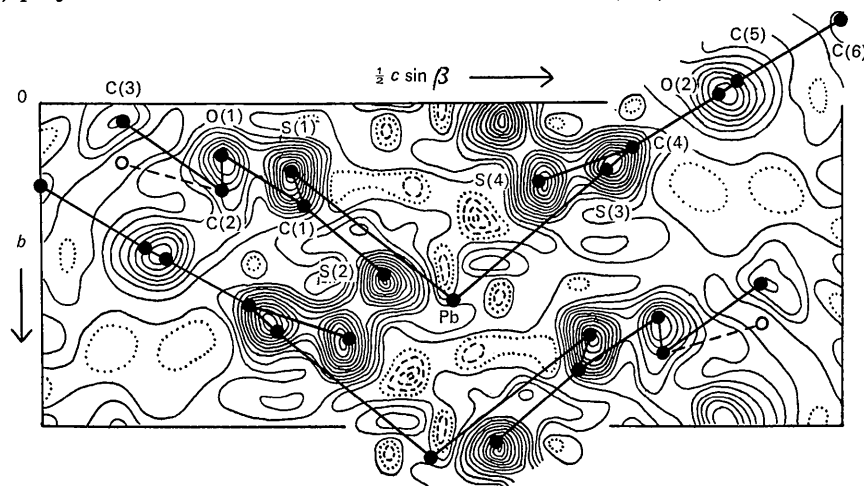


Fig. 3. Difference Fourier projection  $(F_o - F_c)$  on (100), in which the contribution of the lead atom was subtracted. Contours are drawn at intervals of  $2 \text{ e.}\text{\AA}^2$ . Open circles denote atomic positions of C(3), which were determined subsequently by a three-dimensional least-squares refinement with  $h0l$ ,  $h1l$ ,  $h2l$  and  $h3l$  reflexions.

Table 2(a). Observed (FO) and calculated (FC) structure factors

Asterisks denote unobserved reflexions

h	k	l	FO	FC
0	0	0	100	100
0	0	1	100	100
0	0	2	100	100
0	0	3	100	100
0	0	4	100	100
0	0	5	100	100
0	0	6	100	100
0	0	7	100	100
0	0	8	100	100
0	0	9	100	100
0	0	10	100	100
0	0	11	100	100
0	0	12	100	100
0	0	13	100	100
0	0	14	100	100
0	0	15	100	100
0	0	16	100	100
0	0	17	100	100
0	0	18	100	100
0	0	19	100	100
0	0	20	100	100
0	0	21	100	100
0	0	22	100	100
0	0	23	100	100
0	0	24	100	100
0	0	25	100	100
0	0	26	100	100
0	0	27	100	100
0	0	28	100	100
0	0	29	100	100
0	0	30	100	100
0	0	31	100	100
0	0	32	100	100
0	0	33	100	100
0	0	34	100	100
0	0	35	100	100
0	0	36	100	100
0	0	37	100	100
0	0	38	100	100
0	0	39	100	100
0	0	40	100	100
0	0	41	100	100
0	0	42	100	100
0	0	43	100	100
0	0	44	100	100
0	0	45	100	100
0	0	46	100	100
0	0	47	100	100
0	0	48	100	100
0	0	49	100	100
0	0	50	100	100
0	0	51	100	100
0	0	52	100	100
0	0	53	100	100
0	0	54	100	100
0	0	55	100	100
0	0	56	100	100
0	0	57	100	100
0	0	58	100	100
0	0	59	100	100
0	0	60	100	100
0	0	61	100	100
0	0	62	100	100
0	0	63	100	100
0	0	64	100	100
0	0	65	100	100
0	0	66	100	100
0	0	67	100	100
0	0	68	100	100
0	0	69	100	100
0	0	70	100	100
0	0	71	100	100
0	0	72	100	100
0	0	73	100	100
0	0	74	100	100
0	0	75	100	100
0	0	76	100	100
0	0	77	100	100
0	0	78	100	100
0	0	79	100	100
0	0	80	100	100
0	0	81	100	100
0	0	82	100	100
0	0	83	100	100
0	0	84	100	100
0	0	85	100	100
0	0	86	100	100
0	0	87	100	100
0	0	88	100	100
0	0	89	100	100
0	0	90	100	100
0	0	91	100	100
0	0	92	100	100
0	0	93	100	100
0	0	94	100	100
0	0	95	100	100
0	0	96	100	100
0	0	97	100	100
0	0	98	100	100
0	0	99	100	100
0	0	100	100	100



of error. The asymmetry of the structure of the molecule about the lead atom is evidently seen from the positions of S(2) and S(4) atoms. The atom distances Pb-S(2) and Pb-S(4) are  $2.838 \pm 0.025$  and  $2.950 \pm 0.030$  Å respectively, and their difference,  $0.112$  Å, is significant. The asymmetry is still more marked in the atom distances S(2)-S(3) and S(1)-S(4), being  $3.77 \pm 0.04$  Å and  $4.16 \pm 0.04$  Å respectively, the difference,  $0.39$  Å, being definitely significant.

#### Intermolecular distances

The molecules are arrayed in the crystal through twofold screw axes and symmetry centres as shown in Figs. 4 and 5. S(2) and S(2') atoms and S(4) and S(4') atoms come into contact through the twofold screw axes with distances  $3.65 \pm 0.04$  and  $3.59 \pm 0.04$  Å respectively. The difference between them,  $0.06$  Å, is insignificant. The distances are in conformity with the

Table 3. Atom distances, bond angles and their standard deviations

Bond distances			
Pb—S(1)	$2.74 \pm 0.03$ Å	Pb—S(3)	$2.79 \pm 0.03$ Å
C(1)—S(1)	$1.70 \pm 0.11$	C(4)—S(3)	$1.78 \pm 0.10$
C(1)—S(2)	$1.68 \pm 0.11$	C(4)—S(4)	$1.66 \pm 0.10$
C(1)—O(1)	$1.30 \pm 0.12$	C(4)—O(2)	$1.28 \pm 0.14$
O(1)—C(2)	$1.52 \pm 0.14$	O(2)—C(5)	$1.44 \pm 0.18$
C(2)—C(3)	$1.53 \pm 0.18$	C(5)—C(6)	$1.53 \pm 0.18$
Other intramolecular atom distances			
Pb—S(2)	$2.84 \pm 0.03$ Å	Pb—S(4)	$2.95 \pm 0.03$ Å
S(1)—S(2)	$2.98 \pm 0.04$	S(3)—S(4)	$2.94 \pm 0.04$
S(1)—S(4)	$4.16 \pm 0.04$	S(2)—S(3)	$3.77 \pm 0.04$
Intermolecular distances			
van der Waals distance between sulphur atoms			
S(2)—S(2')	$3.65 \pm 0.04$ Å	S(4)—S(4')	$3.59 \pm 0.04$ Å
van der Waals distance between methyl ends of the ethyl groups			
C(3') — C(3'')	$4.30 \pm 0.40$ Å	C(6) — C(6'')	$4.13 \pm 0.30$ Å
C(3', + b)—C(3'')	$3.75 \pm 0.40$	C(6, + b)—C(6'')	$4.47 \pm 0.30$
C(6) — C(3'')	$4.27 \pm 0.25$	C(6, + b)—C(3'')	$4.18 \pm 0.25$
Other intermolecular atom distances			
Pb(-b)—S(1)	$3.32 \pm 0.03$ Å	Pb(-b)—S(3)	$3.37 \pm 0.03$ Å
Pb(-b)—S(2)	$4.81 \pm 0.03$	Pb(-b)—S(4)	$3.50 \pm 0.03$
Bond angles			
	S(1)—Pb—S(3)	$98.2 \pm 0.9^\circ$	
Pb—S(1)—C(1)	$87 \pm 3^\circ$	Pb—S(3)—C(4)	$91 \pm 3^\circ$
S(1)—C(1)—S(2)	$124 \pm 6$	S(3)—C(4)—S(4)	$118 \pm 6$
S(1)—C(1)—O(1)	$113 \pm 7$	S(3)—C(4)—O(2)	$116 \pm 7$
S(2)—C(1)—O(1)	$122 \pm 7$	S(4)—C(4)—O(2)	$127 \pm 7$
C(1)—O(1)—C(2)	$118 \pm 8$	C(4)—O(2)—C(5)	$117 \pm 8$
C(1)—C(2)—C(3)	$108 \pm 8$	O(2)—C(5)—C(6)	$104 \pm 8$

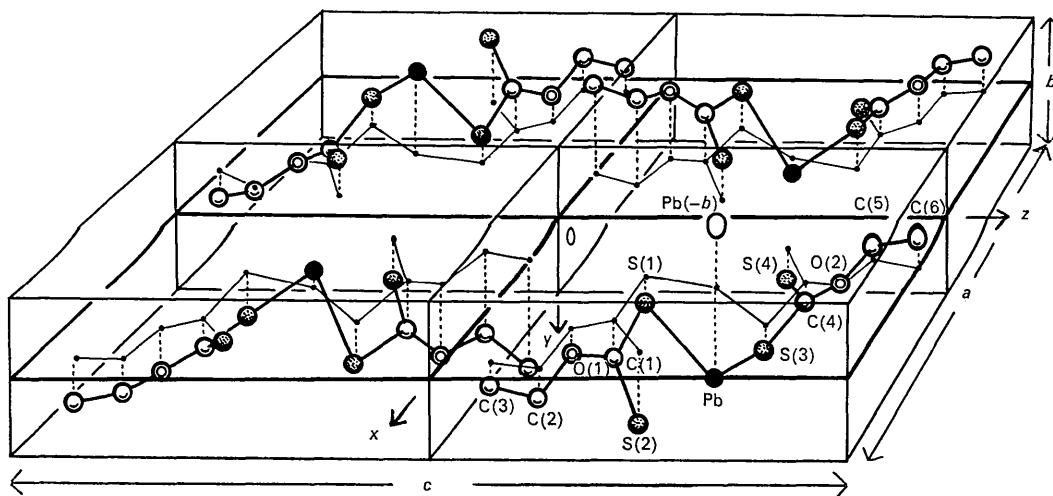


Fig. 4. Representation of the configuration of atoms in the unit cell of lead ethylxanthate. Small dots denote projections of atoms on the plane  $y=0$ .

van der Waals distance of sulphur atoms, 3.70 Å. It is to be noticed that the distances between the Pb(-b) atom in Fig. 4 and S(1), S(2), S(3) and S(4) atoms, listed in Table 3, are definitely larger than the Pb-S bond distances, 2.74 and 2.79 Å, in the present analysis, or the sum of divalent ionic radii of lead and sulphur atoms,  $1.20 + 1.85 = 3.05$  Å. This result indicates that there exists no direct binding between molecules piled up in the *b*-axis direction.

Through symmetry centres the methyl ends of the ethyl groups of the molecules come into contact as shown in Fig. 5. The distances between carbon atoms of the methyl ends are listed in Table 3. They are in conformity with the van der Waals distance, approximately 4.0 Å, of a methyl group. As explained already, the C(3) atom deviates from the plane which is defined by S(1), S(2) and O(1) atoms and which contains C(1) and C(2) atoms. This deviation is interpreted by the rotation of the -C(2)-C(3) segment of the xanthate group around the O(1)-C(2) bond so that the distances between the methyl ends of the neighbouring molecules become nearer to 4.0 Å. In planar configuration they are calculated to be 3.4 Å and 4.9 Å.

#### *A geometrical interpretation of the asymmetric structure of the molecule*

A free lead ethylxanthate molecule is supposed from its composition to have a symmetrical structure, at least with a twofold rotation axis passing through the lead atom. The present result has shown that the molecule is asymmetric in the crystalline state. In the following a geometrical consideration will be given of the deformation which the molecules undergo when they are assembled together to form a crystal.

First, consider a molecular model consisting of two planar ethylxanthate groups connected with a lead atom,  $C(3'')C(2'')O(1'')C(1'')S(2'')S(1)-Pb-S(3)S(4)C(4')O(2'')C(5'')C(6'')$  in Fig. 6. With this model the molecule possesses a twofold rotation axis passing through the lead atom and normal to the plane defined by two xanthate groups. For the bond angle S(1)-Pb-S(3) a value of  $98^\circ$  was adopted, and the following mean values for the other bond distances and angles: Pb-S(1) and Pb-S(3) 2.77 Å, Pb-S(1)-C(1') and Pb-S(3)-C(4')  $89^\circ$ , S(1)-C(1') and S(3)-C(4') 1.74 Å, C(1')-S(2'') and C(4')-S(4'') 1.67 Å, S(1)-C(1')-S(2'') and S(3)-C(4')-S(4'')  $120^\circ$ .

With this model the deviation of the lead atom from the plane defined by two xanthate groups is 1.80 Å, a value definitely larger than those observed with the actual molecule, 0.42 Å with one xanthate group and 0.79 Å with another. When the xanthate group in the model structure is rotated around the C-S single bond, the distance between the lead atom and the plane of the xanthate group is altered. By a rotation  $\varphi_1 = 32^\circ \pm 2^\circ$  in the direction depicted with an arrow in Fig. 6 this distance will be  $0.42 \pm 0.10$  Å. Similarly, by a rotation  $\varphi_2 = 24^\circ \pm 2^\circ$  the distance will be  $0.79 \pm 0.10$  Å. The two xanthate groups thus rotated are depicted with shaded circles in Fig. 6. With these rotations the atom distances Pb-S(2') and Pb-S(4') come out to be 2.92 and 2.97 Å respectively, in fairly good agreement with the result of the analysis: Pb-S(2)  $2.84 \pm 0.03$  Å, Pb-S(4)  $2.95 \pm 0.03$  Å.

There still remain large discrepancies in the atom distances between the molecular model of shaded circles and the actual molecule analysed. The distances S(2')-S(3) and S(1)-S(4') in Fig. 6 come out to be 4.04 and

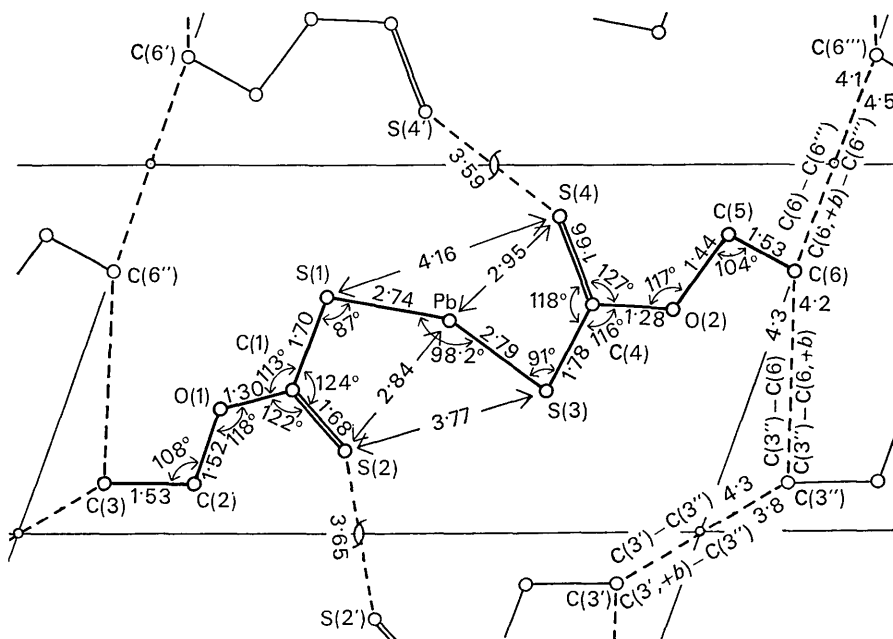


Fig. 5. Atom distances and bond angles of lead ethylxanthate. Notation,  $C(3', +b)$  for example, means C(3) atom brought to  $C(3')$  by the operation of a screw axis and then translated in the  $+y$  direction by an amount  $b$ .



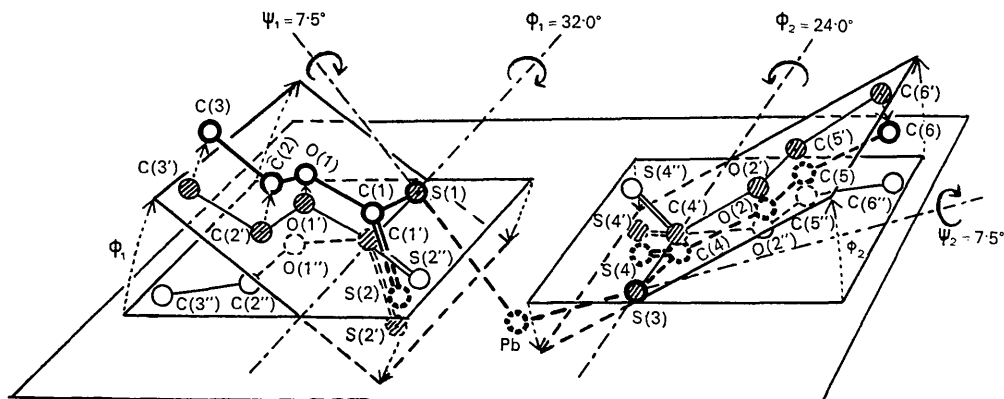


Fig. 6. Representation of the construction of a non-planar asymmetric molecule of lead ethylxanthate from a symmetrical structure by rotations of the molecular segments around C-S and Pb-S single bonds.

3.93 Å respectively, whereas the actual distances analysed are  $S(2)-S(3) = 3.77 \pm 0.04$  Å and  $S(1)-S(4) = 4.16 \pm 0.04$  Å. The discrepancy is removed by the rotation of the xanthate groups, each separately, around the Pb-S(1) and Pb-S(3) bonds. By rotations  $\psi_1 = \psi_2 = 7.5^\circ \pm 2.0^\circ$  in directions depicted with arrows the distances  $S(2)-S(3)$  and  $S(1)-S(4)$  will be  $3.78 \pm 0.07$  and  $4.14 \pm 0.05$  Å respectively, in conformity with the experimental result. In these rotations the distance between the lead atom and each xanthate group plane is unchanged. Also unchanged are the distances Pb-S(2') and Pb-S(4'). The molecular model thus constructed for the explanation of the asymmetric structure of the actual molecule in the crystalline state is depicted with thick circles in Fig. 6.

The reason for these mutually independent rotations of the molecular segments in the crystal is supposed, on the one hand, to be due to the van der Waals attraction between double bonded sulphur atoms,  $S(4) \cdots S(4')$  and  $S(2) \cdots S(2')$ , and on the other to the conditions required for the alkyl groups of the molecules to be packed as closely as possible. The conclusion of the present analysis, that the lead ethylxanthate molecule undergoes deformation through rotations of the molecular segments around Pb-S, C-S and O-C bonds in the crystalline state, is of interest in connection with the interpretation of the result of the electron diffraction study on the structure of the patches of compact monolayers of xanthate adsorbed on galena surfaces (Hagihara, Sakurai & Ikeda, 1964).

The physico-chemical interpretation of the bonding of the lead atom with the sulphur atoms of the dithiocarbonic ends of the xanthate groups will be given shortly together with the result obtained for the structure of lead *n*-butylxanthate crystals.

The present analysis was initiated at the Kobayashi Institute of Physical Research, Kobunzi, Tokyo,

where the two-dimensional analyses were completed, and the authors are especially grateful to Prof. K. Sato, the director of the Institute, for his encouragement. We are also grateful to Dr T. Sakurai of the Institute of Physical Chemical Research, Tokyo, for his valuable aid and discussions.

#### References

- ALBRECHT, G. (1939). *Rev. Sci. Instrum.* **10**, 221.  
 GAUDIN, A. M. (1957). *Flotation*. 2nd ed. New York: McGraw-Hill.  
 HAGIHARA, H. (1952). *J. Phys. Chem.* **56**, 610, 616.  
 HAGIHARA, H. & UCHIKOSHI, H. (1954). *Nature, Lond.* **174**, 80.  
 HAGIHARA, H., UCHIKOSHI, H. & YAMASHITA, S. (1957). *Proc. 2nd Intern. Conf. on Surface Activity*, Vol. 3, 343. London: Butterworths.  
 HAGIHARA, H., SAKURAI, T. & IKEDA, T. (1964). *Proc. 4th Intern. Conf. on Surface Active Substances*, B/III-12, Bruxelles.  
 HOWELLS, R. G. (1950). *Acta Cryst.* **3**, 366.  
*Internationale Tabellen zur Bestimmung von Kristallstrukturen* (1935). Bd. II, *Mathematische u. physikalische Tabellen*. Berlin: Borntraeger.  
 LANDOLT-BÖRNSTEIN (1955). *Physikalische-chemischen Tabellen*, Bd. I/4 *Kristalle*, p. 521. Berlin: Springer.  
 LIPSON, H. & COCHRAN, W. (1953). *The Determination of Crystal Structures*, p. 309. London: Bell.  
 PAULING, L. (1960). *The Nature of the Chemical Bond*. 3rd ed., pp. 221-264. Ithaca: Cornell Univ. Press.  
 TAGGART, A. F. (1947). *Handbook of Mineral Dressing*. New York: John Wiley.  
 WARK, I. W. & SUTHERLAND, K. L. (1955). *Principles of Flotation*. Melbourne: Australasian Institute of Mining & Metallurgy.  
 VAN DEN HENDE, J. H. (1961). *Crystallographic Structure Factor and Least-Squares Refinement Program for the IBM 7090 Computer*. Esso Research & Engineering Co., P.O. Box 45, Linden, N.J., U.S.A.